Forward production of Υ mesons in pp collisions at √s = 7 and 8 TeV

Preliminary results

Alexander Artamonov [1], on behalf of LHCb Collaboration
[1] Institute for High Energy Physics, Protvino, Russia

LHCb-PAPER-2015-045

Presented at The Third Annual Large Hadron Collider Physics Conference (LHCP2015)

1. Introduction

Studies of heavy quarkonium systems, such as the $b\bar{b}$ states, Υ(1S), Υ(2S) and Υ(3S), probe the dynamics of the colliding partons providing insight into the non-perturbative regime of quantum chromodynamics (QCD). Despite many models that have been proposed, a complete description of heavy quarkonium production is still not available. The study of production of heavy quarkonia could help to shed light on this long-standing question.

In this poster we report on the measurement of the inclusive production cross-sections of the Υ states at √s = 7 and 8 TeV and of their ratios. The existing LHCb measurements of these quantities were performed at √s = 7 TeV with a data sample collected in 2010 corresponding to 25 pb^{-1} [1], and at √s = 8 TeV for early 2012 data using about 50 pb^{-1} [2]. Both measurements were differential in p_T and y of the Υ mesons in the ranges 2.0 < y < 4.5 and p_T < 15 GeV/c. Based on these measurements, an increase of the production cross-section in excess of 30% between √s = 7 TeV to 8 TeV was observed, which is larger than the increase observed for other quarkonium states such as the J/ψ [2],[3] and larger than the expectations from NR QCD [4].

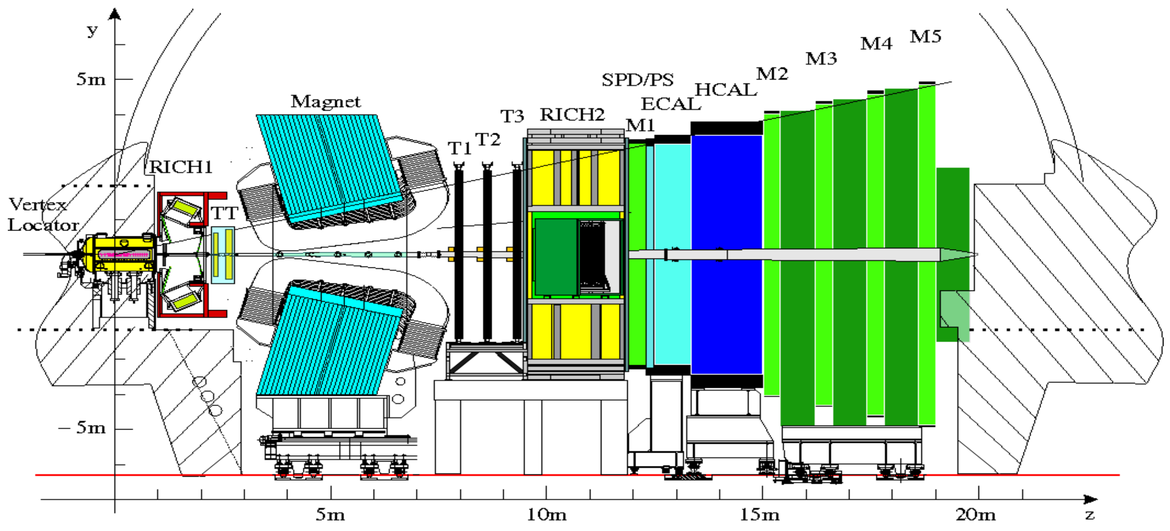

JINST 3 (2008) S08005

Figure: View of the LHCb detector

IJMP A30 (2015) 1530022

2. Dataset and selection

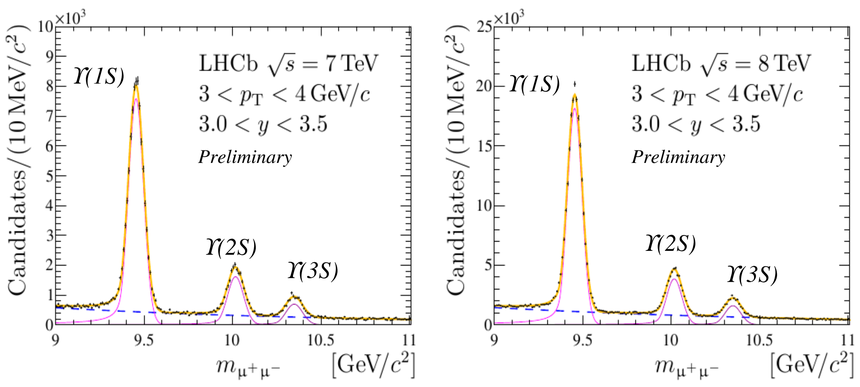

Figure: Efficiency-corrected dimuon mass distribution for √s = 7 TeV (left) and √s = 8 TeV (right) samples in the 3<p_T<4 GeV/c, 3.0<y<3.5 region. The three peaks correspond to the Υ(1S), Υ(2S) and Υ(3S) signals.

- Run-I dataset with $\mathcal{L}$ = 1 fb^{-1} & 2 fb^{-1} of pp collisions at √s = 7 TeV (2011) & 8 TeV (2012)
- Reconstructed using Υ(nS)→μ⁺μ⁻ decay mode, selected in 2.0 < y < 4.5 and p_T < 30 GeV/c
- Measurement performed in bins of p_T and y

$$\mathcal{B}_\Upsilon \times \frac{\mathrm{d}^2}{\mathrm{d}p_T\,\mathrm{d}y}\sigma(pp \to \Upsilon X) \equiv \frac{1}{\Delta p_T \Delta y}\sigma_{\mathrm{bin}}^{\Upsilon\to\mu^+\mu^-} = \frac{1}{\Delta p_T \Delta y}\frac{N_{\Upsilon\to\mu^+\mu^-}}{\mathcal{L}}$$

- Υ(nS) signal extraction performed by unbinned extended maximum likelihood weighted fit (baseline method), crosschecked by the method used in [5] based on the sPlot technique
- In each (p_T,y) bin, the dimuon mass distribution is described by the sum of three Crystall Ball functions, one for each of the Υ(1S), Υ(2S) and Υ(3S) signals, and the product of an exponential function with a second-order polynomial for the combinatorial background

3.1 Differential cross-sections

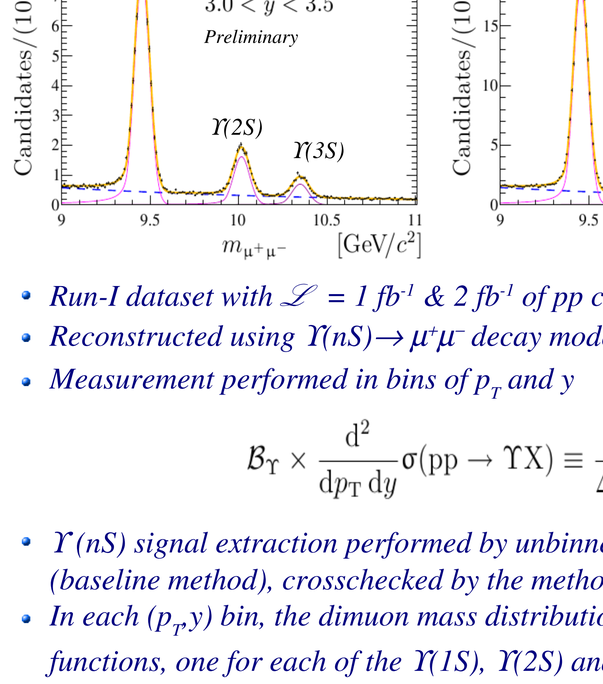

Figure: Double differential cross-sections for √s = 7 TeV (left) and √s = 8 TeV (right) data. Rapidity ranges: 2.0 <y < 2.5, 2.5 < y < 3.0, 3.0 < y < 3.5, 3.5 < y < 4.0, 4.0 < y < 4.5

Table 1: Efficiency-corrected signal yields for data samples accumulated at $\sqrt{s} = 7$ and 8 TeV summed over the full kinematic range $p_T < 30$ GeV/c, $2.0 < y < 4.5$. The uncertainties are statistical only.

Preliminary

	$\sqrt{s} = 7$ TeV	$\sqrt{s} = 8$ TeV
$N_{\Upsilon(1S)\to\mu^+\mu^-}$	$(2639.8 \pm 3.7) \cdot 10^3$	$(6563.1 \pm 6.3) \cdot 10^3$
$N_{\Upsilon(2S)\to\mu^+\mu^-}$	$(667.3 \pm 2.2) \cdot 10^3$	$(1674.3 \pm 3.5) \cdot 10^3$
$N_{\Upsilon(3S)\to\mu^+\mu^-}$	$(328.8 \pm 1.5) \cdot 10^3$	$(786.6 \pm 2.6) \cdot 10^3$

Table 10: The production cross-section $\sigma^{\Upsilon\to\mu^+\mu^-}$ (in pb) for Υ mesons in the full p_T kinematic range $p_T < 30$ GeV/c (left two columns) and reduced p_T range $p_T < 15$ GeV/c (right two columns) for $2.0 \le y < 4.5$. The first uncertainties are statistical and the second systematic.

Preliminary

	$p_T < 30$ GeV/c		$p_T < 15$ GeV/c	
	$\sqrt{s} = 7$ TeV	$\sqrt{s} = 8$ TeV	$\sqrt{s} = 7$ TeV	$\sqrt{s} = 8$ TeV
$\sigma^{\Upsilon(1S)\to\mu^+\mu^-}$	$2510 \pm 3 \pm 80$	$3280 \pm 3 \pm 100$	$2460 \pm 3 \pm 80$	$3210 \pm 3 \pm 90$
$\sigma^{\Upsilon(2S)\to\mu^+\mu^-}$	$635 \pm 2 \pm 20$	$837 \pm 2 \pm 25$	$614 \pm 2 \pm 20$	$807 \pm 2 \pm 24$
$\sigma^{\Upsilon(3S)\to\mu^+\mu^-}$	$313 \pm 2 \pm 10$	$393 \pm 1 \pm 12$	$298 \pm 1 \pm 10$	$373 \pm 1 \pm 11$

3.2 Differential cross-sections

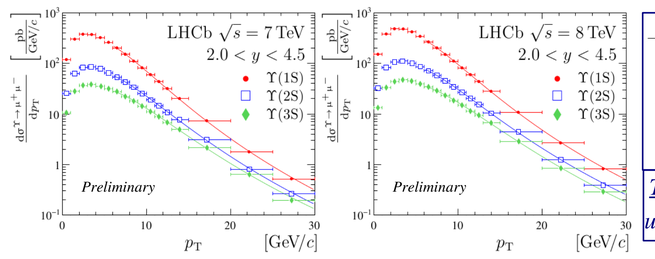

	$\sqrt{s}$	T [GeV]	n
Υ(1S)	7 TeV	1.19 ± 0.04	8.01 ± 0.33
	8 TeV	1.20 ± 0.04	7.71 ± 0.27
Υ(2S)	7 TeV	1.33 ± 0.05	7.57 ± 0.41
	8 TeV	1.37 ± 0.05	7.53 ± 0.34
Υ(3S)	7 TeV	1.53 ± 0.07	7.85 ± 0.56
	8 TeV	1.63 ± 0.06	8.23 ± 0.51

Table: Results of the fits to the p_T spectra of Υ mesons using the Tsallis function in 6 < p_T < 30 GeV/c

Tsallis function, $\frac{\mathrm{d}\sigma}{p_T \mathrm{d}p_T} \propto \left(1 + \frac{E_T^{\mathrm{kin}}}{nT}\right)^{-n}$, to fit the p_T spectra in 6 < p_T < 30 GeV/c

Figure: Differential cross-sections, dσ/dp_T, in the range 2.0<y<4.5 for Υ mesons for √s = 7 TeV (left) and √s = 8 TeV data. The curves show the fit results with the Tsallis function. The fitted values of the parameters n and T are listed in Table below. The fitted values of the parameter n for all cases are close to 8, compatible with the high-p_T asymptotic behaviour expected by the colour-singlet model [PR D23 (1981) 1521, NP B172 (1980) 425, ZP C19 (1983) 251].

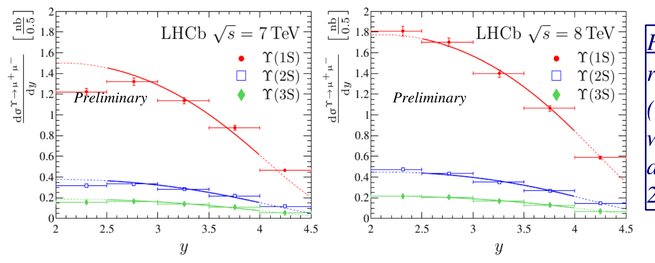

Figure: Differential cross-sections, dσ /dy , in the range p_T < 30 GeV/c for Υ mesons for √s = 7 TeV (left) and √s = 8 TeV data. Thick lines show fit results with the colour-octet model predictions in 2.5<y<4.0, and dashed lines show extrapolation to the full 2.0<y<4.5 region.

4. Production ratios

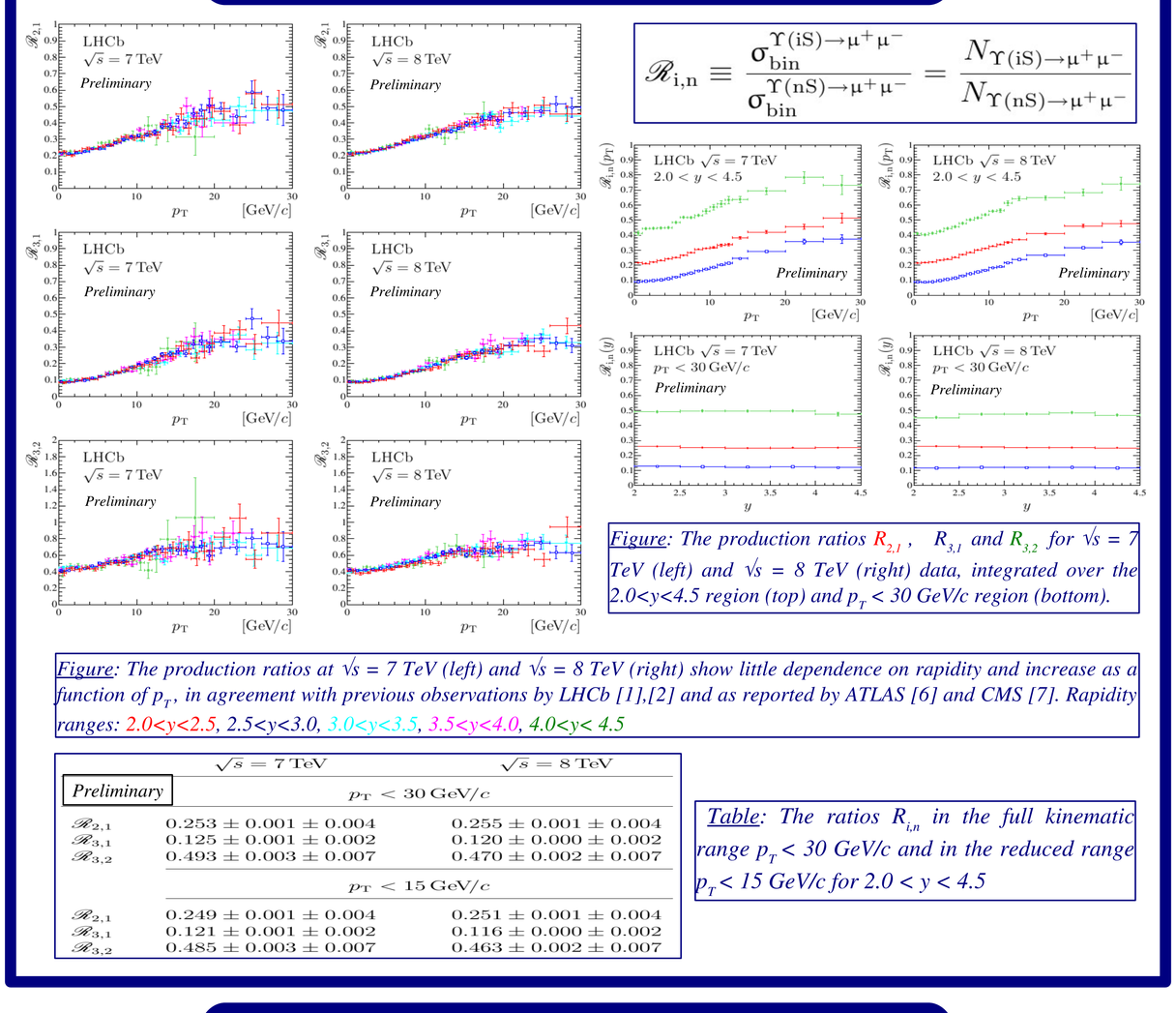

$$\mathcal{R}_{i,n} \equiv \frac{\sigma_{\mathrm{bin}}^{\Upsilon(iS)\to\mu^+\mu^-}}{\sigma_{\mathrm{bin}}^{\Upsilon(nS)\to\mu^+\mu^-}} = \frac{N_{\Upsilon(iS)\to\mu^+\mu^-}}{N_{\Upsilon(nS)\to\mu^+\mu^-}}$$

Figure: The production ratios $R_{2,1}$, $R_{3,1}$ and $R_{3,2}$ for √s = 7 TeV (left) and √s = 8 TeV (right) data, integrated over the 2.0<y<4.5 region (top) and p_T < 30 GeV/c region (bottom).

Figure: The production ratios at √s = 7 TeV (left) and √s = 8 TeV (right) show little dependence on rapidity and increase as a function of p_T, in agreement with previous observations by LHCb [1],[2] and as reported by ATLAS [6] and CMS [7]. Rapidity ranges: 2.0<y<2.5, 2.5<y<3.0, 3.0<y<3.5, 3.5<y<4.0, 4.0<y< 4.5

Preliminary

	$\sqrt{s} = 7$ TeV	$\sqrt{s} = 8$ TeV
	$p_T < 30$ GeV/c	
$\mathcal{R}_{2,1}$	$0.253 \pm 0.001 \pm 0.004$	$0.255 \pm 0.001 \pm 0.004$
$\mathcal{R}_{3,1}$	$0.125 \pm 0.001 \pm 0.002$	$0.120 \pm 0.000 \pm 0.002$
$\mathcal{R}_{3,2}$	$0.493 \pm 0.003 \pm 0.007$	$0.470 \pm 0.002 \pm 0.007$
	$p_T < 15$ GeV/c	
$\mathcal{R}_{2,1}$	$0.249 \pm 0.001 \pm 0.004$	$0.251 \pm 0.001 \pm 0.004$
$\mathcal{R}_{3,1}$	$0.121 \pm 0.001 \pm 0.002$	$0.116 \pm 0.000 \pm 0.002$
$\mathcal{R}_{3,2}$	$0.485 \pm 0.003 \pm 0.007$	$0.463 \pm 0.002 \pm 0.007$

Table: The ratios $R_{i,n}$ in the full kinematic range p_T < 30 GeV/c and in the reduced range p_T< 15 GeV/c for 2.0 < y < 4.5

5. Ratios of cross-sections

Preliminary

	$p_T < 30$ GeV/c	$p_T < 15$ GeV/c
Υ(1S)	$1.307 \pm 0.002 \pm 0.025$	$1.304 \pm 0.002 \pm 0.024$
Υ(2S)	$1.319 \pm 0.005 \pm 0.025$	$1.315 \pm 0.005 \pm 0.024$
Υ(3S)	$1.258 \pm 0.007 \pm 0.024$	$1.254 \pm 0.007 \pm 0.023$

$$\mathcal{R}_{8/7} \equiv \frac{\sigma_{\mathrm{bin}}^{\Upsilon\to\mu^+\mu^-}\Big|_{\sqrt{s}=8\ \mathrm{TeV}}}{\sigma_{\mathrm{bin}}^{\Upsilon\to\mu^+\mu^-}\Big|_{\sqrt{s}=7\ \mathrm{TeV}}}$$

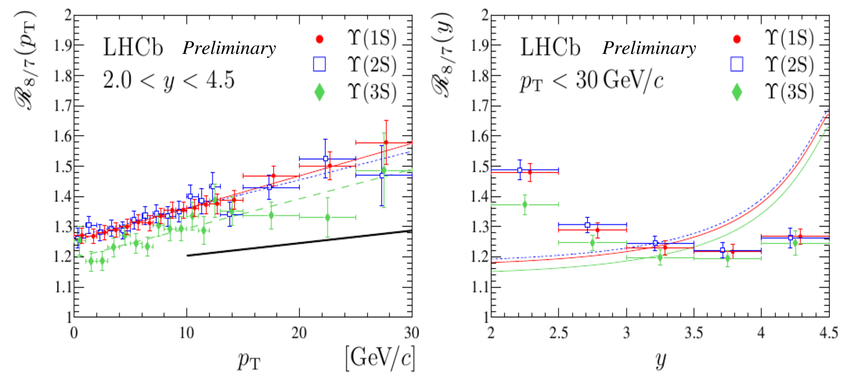

Figure: Ratios of differential cross-sections (left) dσ/dp_T and (right) dσ/dy at √s = 8 TeV & √s = 7 TeV for Υ(1S), Υ(2S) and Υ(3S). On the left plot, the results of the fit with a linear function are shown. In the same plot, the NLO NR QCD theory predictions [4] are shown as a thick line. On the right plot, the curved lines show the colour-octet model predictions [Phys.Rev.D84(2011)114020, MPL A29 (2014) 1450082].

6. References

[1] LHCb collaboration, R.Aaij et al., Eur. Phys. J. C72 (2012) 2025
[2] LHCb collaboration, R.Aaij et al., JHEP 06 (2013) 064
[3] LHCb collaboration, R.Aaij et al., Eur. Phys. J. C71 (2011) 1645
[4] H.Han et al., arXiv:1410.8537
[5] LHCb collaboration, R.Aaij et al., Eur. Phys. J. C74 (2014) 2835
[6] ATLAS collaboration, G.Aad et al., Phys. Rev. D87 (2013) 052004
[7] CMS collaboration, V.Kachatryan et al., Phys. Rev. D83 (2011) 112004